

Direct Observation of Excited State Conversion in Solid State from a TICT-Type Mechanochromic Luminogen

Jianai Chen¹, Sijie Tan¹, Yue Yu¹, Shitong Zhang², Weijun Li¹, Qingbao Song¹, Yujie Dong^{1*},
Cheng Zhang^{1*}, and Wai-Yeung Wong^{3*}

¹State Key Laboratory Breeding Base of Green Chemistry Synthesis Technology, College of Chemical Engineering, Zhejiang University of Technology, Hangzhou 310014, P. R. China.

²State Key Lab of Supramolecular Structure and Materials, Jilin University, 2699 Qianjin Avenue, Changchun 130012, P. R. China.

³Department of Applied Biology & Chemical Technology, The Hong Kong Polytechnic University, Hung Hom, Hong Kong, P. R. China; Hong Kong Polytechnic University Shenzhen Research Institute, Shenzhen 518057, P.R. China.

Corresponding authors: dongyujie@zjut.edu.cn, czhang@zjut.edu.cn and wai-yeung.wong@polyu.edu.hk

Abstract

A coplanar donor-acceptor (D-A) structure in single crystal is directly observed for TICT-Type DPA-PYZ, which corresponds to a coplanar localized excited (LE) state. The conversion between coplanar LE and twisted intramolecular charge transfer (TICT) excited state in the solid state can be achieved through the change of the D-A twist angle between $\sim 0^\circ$ and $\sim 30^\circ$ during grinding, heating and solvent fumigation processes. This twist angle change between donor and acceptor was proved by the Raman, FT-IR spectroscopy and X-ray crystallographic analysis as well as theoretical calculation. This research provides the clear evidence for the conversion between coplanar LE and TICT excited states of D-A molecules in solid state and contributes much to the deep understanding of stimulus-response behavior of fluorescent D-A molecular solids from the viewpoint of excited state control.

KEYWORDS: coplanar D-A structure, TICT, triphenylamine, solid-state luminescence, excited state conversion, mechanochromism.

1. Introduction

Solid-state luminescent materials have attracted great interests in recent years, due to the practical requirements of their applications in optoelectronic areas such as organic light-emitting diodes,^[1-6] stimulus response,^[7-11] chemical sensing^[12] and so on. Among them, the donor-acceptor (D-A) luminescent molecules have been attracting much attention due to their twisted construction between donor and acceptor groups, which is vulnerable to the external environments such as solvent polarity and temperature.^[4-7] Owing to this twisted construction, D-A luminescent molecules might generate two different excited states, i.e., a twisted intramolecular charge transfer (TICT) excited state based on a relatively large twist angle and a coplanar localized excited (LE) state based on the twist angle of nearly zero.^[6, 13] This special

property of different excited states for D-A molecules has been deeply studied in the past 20 years. ^[3-6, 14-16]In most cases, luminescence from LE state and TICT excited state could be observed individually or simultaneously in solution according to the different polarities of solvents. ^[16-18]When it comes to the solid-state, the environmental polarity becomes difficult to be quantified and controlled, and fast energy transfer process could also quench the emission from high-energy excited state. Although some molecules with LE-emission in solid state such as phenothiazine derivatives have been reported recently^[19,20], luminescence from the two excited states in solid state is still difficult to be observed, especially for the relatively high-energy LE state emission. ^[4, 5]

Mechanochromic luminogen with typical solid-state switched luminescence characteristics (eg. fluorescence spectra have a large shift under mechanical stimuli), should be as the ideal research object of excited state in the solid state. Recently, the in-depth discussion on ICT-Type molecules with mechanical stimulus-response behaviour have found that the fluorescence color change is highly depended on the conversion of excited states caused by twist angle changes between donor and acceptor.^[11, 14] However, these proposed deduction were mostly based on spectroscopic tests and theoretical calculation, because it is difficult to obtain suitable single crystals which could demonstrate accurate molecular configuration to provide corresponding excited state information. Up to now, in the solid state of mechanochromic TICT-Type molecules, directly clear observation of the conversion between coplanar LE state and TICT excited state is still challenging due to the lack of direct evidence of coplanar D-A molecular configuration with LE state.

Herein, we clearly observed the conversion between coplanar LE state and TICT excited state in the solid state from a diphenylamine-benzoylimino-based mechanochromic D-A molecule DPA-PYZ. The coplanar LE state was found in the crystal structure with the D-A twist angle of nearly zero, while the TICT excited state was observed at the amorphous state with a D-A twist angle of $\sim 30^\circ$. The interconversion between two excited states can be achieved by the grinding, heating and solvent fumigation processes. The LE and TICT states display different fluorescence emissions with λ_{max} at 454 nm and 551 nm respectively, which enables the DPA-PYZ solid to be a typical mechanofluorochromic material with the large spectral shift of ~ 100 nm. This research provides the direct evidence for the conversion between coplanar LE state and TICT excited state of D-A molecules in the solid state and contributes much to the deep understanding of stimulus-response behavior of mechanochromic luminogen from the viewpoint of excited state control.

2. Experimental Section

2.1 Materials and Characterizations

Materials: Benzil ($\text{C}_{14}\text{H}_{10}\text{O}_2$, 98%), aniline ($\text{C}_6\text{H}_7\text{N}$, 99.5%), ammonium acetate ($\text{C}_2\text{H}_7\text{NO}_2$, $\geq 98\%$), acetic acid glacial ($\text{C}_2\text{H}_4\text{O}_2$, $\geq 99.5\%$), 4-(*N,N*-diphenylamino)benzaldehyde ($\text{C}_{19}\text{H}_{15}\text{NO}$, 98%), 4-bromobenzaldehyde ($\text{C}_7\text{H}_5\text{BrO}$, 98%) and *N*-bromosuccinimide ($\text{C}_4\text{H}_4\text{BrNO}_2$, 99%) were purchased from Energy Chemical. Tetrakis (triphenylphosphine)platinum ($\text{Pd}[\text{P}(\text{C}_6\text{H}_5)_3]_4$, $\text{Pd} \geq 8.9\%$), potassium carbonate (K_2CO_3 , $\geq 99\%$), methylbenzene (C_7H_8 , $\geq 99.5\%$), tetrahydrofuran ($\text{C}_4\text{H}_8\text{O}$, $\geq 99.5\%$), 2-isopropoxy-4,4,5,5-tetramethyl-1,3,2-dioxaborolane ($\text{C}_9\text{H}_{19}\text{BO}_3$, 98%) and *n*-butyllithium ($\text{C}_4\text{H}_9\text{Li}$, 2.4 M) were obtained from Aladdin. All the chemicals were used as received without further purification.

Characterizations: The ^1H NMR spectra of the synthesized compounds were recorded on Bruker AVANCE III instrument (Bruker, Switzerland) by utilizing deuterated dimethyl sulfoxide (DMSO) as solvents and tetramethylsilane (TMS) as a standard. The MALDI-TOF mass spectra were recorded using an AXIMA CFRTM plus instrument. Fluorescence measurements were carried out with a RF-5301PC instrument. X-ray diffraction was carried out with X'Pert Pro instrument. The single crystal structure was carried out with an Agilent Gemini instrument. The Raman spectra were carried out with a LabRAM HR UV 800 instrument. The FT-IR spectra were carried out with a Nicolet 6700 instrument. The fluorescence lifetime measurement were carried out in a FLS980 Spectrometer with the InGaAs PDA NIR detector. All measurements were carried out at room temperature under ambient conditions.

2.2 Synthesis

The synthetic routes of TPA-PYZ, DPA-PYZ in Scheme S1 (Supporting Information). They were synthesized according to literatures.^[21] All the target compounds were characterized by ^1H NMR, mass spectrometry analysis.

Synthesis of (*Z*)-*N*-(benzoylimino)(4-(diphenylamino)phenyl)-*N*-phenylbenzamide (DPA-PYZ). The preparation procedure of DPA-PYZ could be found in the reference.^[21] It was synthesized by a photo-chemical reaction in which imidazole ring of DPA-PIM (0.10 g, 0.19 mmol) in methylbenzene was opened to generate the highly luminescent benzoylimino group under UV by O_2 for 4 days. After the solvent had been removed, the residue was purified by column chromatography on silica gel using petroleum ether/ethyl acetate as the eluent to give a yellow solid. (40.0 mg, 38%). ^1H NMR (500 MHz, DMSO- d_6) δ 7.63 (d, J = 8.9 Hz, 2H), 7.62 – 7.55 (m, 4H), 7.51 (t, J = 7.4 Hz, 1H), 7.43 – 7.28 (m, 9H), 7.22 (ddd, J = 17.9, 15.3, 7.3 Hz, 6H), 7.09 (dd, J = 7.6, 6.5 Hz, 5H), 6.75 (d, J = 8.9 Hz, 2H). MS (ESI): MW 571.2, m/z 573.6 (M^+).

Anal. Calcd for C₃₉H₂₉N₃O₂: C, 81.94; H, 5.11; N, 7.35; Found: C, 81.68; H, 5.29; N, 7.15.

[CCDC 1961347]

Synthesis of (Z)-N-((benzoylimino)(4'-(diphenylamino)-[1,1'-biphenyl]-4-yl)methyl)-N-phenylbenzamide (TPA-PYZ). The preparation procedure of TPA-PYZ could be found in the reference.^[21] It was synthesized by a photo-chemical reaction in which TPA-PIM (0.10 g, 0.16 mmol) in methylbenzene was illuminated under UV by O₂ for 4 days. After the solvent had been removed, the residue was purified by column chromatography on silica gel using petroleum ether/ethyl acetate as the eluent to give a yellow solid. (35.0 mg, 34%). ¹H NMR (500 MHz, DMSO-d₆) δ 7.79 (d, J = 8.5 Hz, 2H), 7.70 – 7.63 (m, 6H), 7.61 (d, J = 8.7 Hz, 2H), 7.55 (t, J = 7.4 Hz, 1H), 7.41 (q, J = 7.4 Hz, 3H), 7.38 – 7.29 (m, 8H), 7.27 (t, J = 7.9 Hz, 2H), 7.12 (dd, J = 18.1, 7.4 Hz, 3H), 7.09 – 7.04 (m, 4H), 6.99 (d, J = 8.7 Hz, 2H). MS (ESI): MW 647.3, m/z 649.0 (M⁺). Anal. Calcd for C₃₉H₂₉N₃O₂: C, 81.94; H, 5.11; N, 7.35; Found: C, 81.68; H, 5.29; N, 7.15. [CCDC 1961349]

3. Results and Discussion

3.1 Optical Properties

Two D-A molecules of DPA-PYZ and TPA-PYZ, based on (Z)-N-((benzoylimino)(phenyl)methyl)-N-phenylbenzamide (PYZ) as the acceptor and diphenylamine (DPA) or triphenylamine (TPA) as the donor (Figure 1), were obtained via a new photochemical reaction of their corresponding imidazole derivatives as shown in Scheme S1.^[21] DFT results demonstrate that DPA-PYZ and TPA-PYZ both adopt the molecular configuration with relatively large twist angles between donor and acceptor part (Figure 1). For the optimized geometry in the ground state, the twist angle of DPA-PYZ and TPA-PYZ is estimated to be about 30° and 40°, while for their excited state, the corresponding twist angle is estimated to be

about 55° (DPA-PYZ) and 32° (TPA-PYZ), in Figure S2, respectively. Their separated HOMO and LUMO distributions on donor and acceptor parts indicate the existence of charge transfer transition for both DPA-PYZ and TPA-PYZ in their excited state (Figure S1). The large solvatochromic redshifts of their PL spectra in different polar solvents (Figure S3) further confirmed the existence of charge transfer excited state with large dipole moments.^[4] Thus DPA-PYZ and TPA-PYZ should possess the TICT and ICT characteristics in their lowest excited state, respectively.^[5]

Fluorescent spectra reveal that DPA-PYZ and TPA-PYZ with the similar benzoylimino-benzamide structure display the similar emission (Figure 2a). Compared to PL spectra of DPA-PYZ in film and solution with λ_{\max} at 550 nm and 580 nm respectively, those of TPA-PYZ show some red-shifts with λ_{\max} at 570 nm and 615 nm respectively, while their UV spectra exhibit the inverse spectra shift (Figure S4), which might be attributed to the better conjugation of DPA-PYZ and the larger dipole moment of TPA-PYZ owing to its additional phenyl group. When it comes to the crystalline state, it is surprising that DPA-PYZ and TPA-PYZ display completely different emission colors. As shown in Figure 2b, TPA-PYZ crystal exhibits an expected yellow emission with λ_{\max} at 535 nm, while DPA-PYZ crystal displays an unusual blue emission with λ_{\max} at 455 nm which shows a large blue-shift of ~100 nm in comparison to that in its film. This result is a bit confusing and let us take a deep research into their crystal structures.

3.2 Crystal Structures

Single crystals of both DPA-PYZ and TPA-PYZ were obtained by the vapor diffusion method in the mixed solvents of chloroform- and tetrahydrofuran-methanol, respectively. As shown in Figure S7, in DPA-PYZ and TPA-PYZ crystal structures, the distance of neighboring molecules is so large that there are no obvious strong intermolecular π - π interactions but some

weak C-H- π interactions. Thus, the large difference of DPA-PYZ PL spectra between crystal and film does not derive from the intermolecular packing structure, but more related to their molecular configuration difference between donor and acceptor groups.

It is well-known that the twist angle between donor and acceptor groups in D-A molecules plays a key role in their charge transfer excited state and photoluminescent properties.^[3, 6] This let us focus on the D-A twist angles of DPA-PYZ and TPA-PYZ molecules in their crystal structures. As shown in Figure 3, TPA-PYZ molecule adopts the twisted D-A configuration with twist angles of $\sim 32^\circ$ between TPA donor and PYZ acceptor, and the TPA donor group possesses a common torsional three-blade-propeller structure with the bond angles of 119° - 121° between adjacent C-N bonds. It is unexpected that, in DPA-PYZ, the twist angle between DPA donor and PYZ acceptor was measured to be $\sim 3^\circ$ (very close to 0°), in which the C-N-C plane (highlighted in blue color in Figure 3) in the DPA group is nearly coplanar to the phenyl plane in PYZ group. The coplanar D-A configuration can be observed more obviously from the simplified molecular structure of DPA-PYZ in Figure 3, in which the peripheral torsional phenyl substituents are ignored. The coplanar D-A molecular configuration in DPA-PYZ crystal will produce the LE state emission of DPA-PYZ molecule, which is higher in energy than the corresponding TICT excited state, according to the case of typical TICT molecule DMABN extensively studied in the past decades.^[6] As far as we know, the present crystal with almost totally coplanar D-A configuraion is very rare among TICT mechanochromic molecules. Considering the large PL spectral difference of DPA-PYZ between its film and crystal states, DPA-PYZ molecules in the film might adopt the twisted D-A configuration with the TICT state. As for TPA-PYZ, it should adopt the twisted D-A configuration in film similar to that in crystal. Thus it can be supposed that the large difference of DPA-PYZ PL spectra between crystal and film should be ascribed to

the excited state transformation between LE and TICT state of DPA-PYZ molecule, which arises from the D-A twist angle change from 0° to 30° between DPA and PYZ.

3.3 Theoretical Calculations

In order to further prove the effect of twist angle on the excited state properties of DPA-PYZ molecule, the theoretical calculation of natural transition orbitals (NTO) for the $S_0 \rightarrow S_1$ excitation at td-m062x/6-31g (d, p) level and their corresponding excitation energy for DPA-PYZ molecule with different twist angles between DPA donor and PYZ acceptor was carried out as shown in Figure 4. When the twist angle is set to be $\sim 1^\circ$, the D-A structural conformation of DPA-PYZ is close to be coplanar. The hole and particle are delocalized over the whole molecule, which surely reveals a LE state character. With the twist angle increasing, holes tend to be mainly localized at the DPA donor part and particles mainly at the PYZ acceptor part, which surely reveals the charge transfer excited state character. When the twist angle reaches up to 80° , the hole and particle almost realize the complete separation of electron clouds with a pure charge transfer excited state character. During the change of D-A twist angles from 1° to 80° , a gradually decreased excitation energy for hole \rightarrow particle transition is focused (Figure 4), which indicates that the LE transition in the coplanar D-A configuration possesses the higher-energy luminescence than the charge transfer transition in the DPA-PYZ molecule with the large twist angles. These are consistent with the observed PL spectra of the DPA-PYZ, in which the crystal with the coplanar D-A configuration displays a blue-shifted emission in comparison to the film with the twisted D-A configuration. The theoretical calculation results demonstrate that the twist angle change between DPA donor and PYZ acceptor could bring the excited state transformation between TICT and LE states and further induce the large luminescence difference of DPA-PYZ molecule.

3.3 Spectroscopy

In order to further evaluate the twist angle change of DPA-PYZ molecule between blue-emissive crystal and yellow-emissive powder, the Raman spectra of DPA-PYZ and TPA-PYZ in different solid states were measured. As shown in Figure 5, DPA-PYZ crystal exhibits a double peak at 1588 cm^{-1} and 1603 cm^{-1} , while its yellow-emission powder exhibits a blue-shifted spectrum with the wavenumbers locating at 1591 cm^{-1} (similar to that of TPA-PYZ crystal) and 1614 cm^{-1} , respectively. It is well known that the Raman signals around 1600 cm^{-1} are usually from the breathing vibration of benzene in triphenylamine^[22-24] (Table S1). Therefore, the shifted Raman spectrum should be associated with the structural difference of the triphenylamine part in different solid morphology of DPA-PYZ. According to the above crystal analysis, triphenylamine part in DPA-PYZ crystal shows a coplanar structure (very close to 0°), while that of TPA-PYZ crystal exhibits a torsional three-blade-propeller configuration (30° - 40°). Considering the signal of 1591 cm^{-1} in DPA-PYZ powder is highly similar to that of TPA-PYZ crystal, the blue-shifted Raman signal from 1588 cm^{-1} (crystal) to 1591 cm^{-1} (powder) for DPA-PYZ should be attributed to the structural change of triphenylamine from the coplanar structure to the torsional three-blade-propeller configuration. As for the other blue-shifted Raman signal from 1603 cm^{-1} (crystal) to 1614 cm^{-1} (powder) in DPA-PYZ case, it should be mainly ascribed to the change of aggregation structure from crystal to amorphous state. Moreover, the IR spectra of DPA-PYZ crystal and powder are similar in most peaks except for the C-N stretching from the TPA moieties^[25-27] as shown in Figure S9, which shift from 1299 cm^{-1} for the crystal to 1293 cm^{-1} for the yellow-emissive powder. The IR peak at 1293 cm^{-1} for the yellow-emissive DPA-PYZ powder could also be found in both TPA-PYZ crystal and powder with similar peak shape and position. These data demonstrate the fact that DPA-PYZ molecules in the yellow-emissive film should adopt the twisted D-A molecular configuration and the common TPA unit with a torsional

three-blade-propeller configuration similar to that in the TPA-PYZ crystal. Thus, it is concluded that the most important difference between blue-emissive crystal and yellow-emissive powders of DPA-PYZ is the twist angle change from 0° to 30° between DPA and PYZ unit. (Figure 6a), which results in their different excited state properties and thus fluorescent color.

3.3 Mechanochromism

For DPA-PYZ molecule, two kinds of powders with blue and yellow emission could be obtained simultaneously via physical interconversion. The blue-emissive powder could be obtained by recrystallization method in a mixed tetrahydrofuran/water solution of DPA-PYZ, while the yellow-emissive powder could be obtained. The PXRD results in Figure S10 demonstrate that the yellow-emissive powder of DPA-PYZ possesses the amorphous aggregated structure, while the blue-emitting one displays the crystalline aggregated structure, consistent with the simulated XRD peaks from the single crystal, which indicates the blue-emissive powder of DPA-PYZ adopts the same molecular configuration and packing mode as its single crystal.

Actually, the yellow-emissive amorphous powder of DPA-PYZ could also be transformed directly from the blue-emissive crystalline one by grinding, and the blue-emission could recover after the heating or solvent fumigation process. As shown in Figure 6b, a yellow-light word “ZJUT” could be written on the blue-light film of DPA-PYZ, then after fuming with DCM vapor or annealing under 60°C , the yellow light word “ZJUT” would disappear with the film recovering back to blue-light. High T_d of $\sim 250^\circ\text{C}$ for DPA-PYZ (Figure S11) enabled the good thermal stability of its film during the 60°C annealing process. The DPA-PYZ molecule thus belongs to the mechanochromic materials^[28-30]. The reversible mechanochromic PL spectra shift is as large as 100 nm between 438 nm and 540 nm (Figure 6c, d), which is among the best reported results for mechanochromic materials^[31-33].

In the mechanochromic process, the gradual transformation of molecular structure and packing mode from blue-emissive crystalline state to yellow-emissive amorphous state was observed in PXRD (Figure S12), and the IR spectra showed the corresponding gradual changes at around 1299 cm^{-1} (Figure S13). Upon mechanical grinding, the Raman spectra of DPA-PYZ also shifted around 1588 cm^{-1} (Figure S14), while as contrast, that of TPA-PYZ didn't change significantly (Figure S15). The gradual change from blue-emissive powder to yellow-emissive one makes us clearly observe the molecular structural transformation during the mechanochromic process.

3.3 Conclusions

In summary, we obtained a novel mechanochromic D-A molecule (DPA-PYZ) with two different fluorescence colors of yellow and blue in its solid states. The blue emission of DPA-PYZ exists in crystalline solid and is attributed to the higher-energy LE state corresponding to coplanar D-A configuration, while the yellow emission occurs in the amorphous solid and is ascribed to the TICT excited state corresponding to a highly twisted D-A configuration. As far as we know, this is the first observation of coplanar D-A structure in single crystal in the mechanochromic molecular cases. Through the Raman, FT-IR spectroscopy, X-ray crystallographic analysis and theoretical calculation, it was confirmed that the biggest difference between the blue- and yellow-emissive powders of DPA-PYZ is the D-A twist angle in molecular structure. The conversion of excited states between LE and TICT state corresponding to structural transformation in the solid state was also observed during the grinding, heating and solvent fumigation processes. In addition, DPA-PYZ is a reversible mechanochromic material with large spectral shift of nearly 100 nm, which is among the best results ever reported. This research provides the clear evidence for the conversion between coplanar LE and TICT excited

states of D-A molecules in the solid state and contributes to the deep understanding of stimulus-response behavior of D-A molecular solids from the viewpoint of excited state manipulation.

Acknowledgments

Thanks to financial supports from National Natural Science Foundation of China (51603185, 51673174, 51803071, 21875219) and Zhejiang Provincial Natural Science Foundation of China (LY19E030006, LQ19E030016, LZ17E030001). W.-Y. W. would like to thank the National Natural Science Foundation of China (51873176), Hong Kong Research Grants Council (PolyU 153058/19P and C6009-17G), Hong Kong The acknowledgements come at the end of an article after the conclusions and before the notes and references. Polytechnic University (1-ZE1C) and The Endowed Professorship in Energy from Ms. Clarea Au (847S) for the financial support.

References

- [1] Penfold, T. J.; Dias, F. B.; Monkman, A. P. The theory of thermally activated delayed fluorescence for organic light emitting diodes. *Chem. Commun.* **2018**, *54*, 3926-3935.
- [2] Liu, H.; Yao, L.; Li, B.; Chen, X.; Gao, Y.; Zhang, S.; Li, W.; Lu, P.; Yang, B.; Ma, Y. Excimer-induced high-efficiency fluorescence due to pairwise anthracene stacking in a crystal with long lifetime. *Chem. Commun.* **2016**, *52*, 7356-7359.
- [3] Li, W.; Liu, D.; Shen, F.; Ma, D.; Wang, Z.; Feng, T.; Xu, Y.; Yang, B.; Ma, Y. A twisting donor-acceptor molecule with an intercrossed excited state for highly efficient, deep-blue electroluminescence. *Adv. Funct. Mater.* **2012**, *22*, 2797-2803.
- [4] Li, W.; Pan, Y.; Xiao, R.; Peng, Q.; Zhang, S.; Ma, D.; Li, F.; Shen, F.; Wang, Y.; Yang, B.; Ma, Y. Employing ~100% excitons in oleds by utilizing a fluorescent molecule with hybridized local and charge-transfer excited state. *Adv. Funct. Mater.* **2014**, *24*, 1609-1614.

- [5] Li, W.; Pan, Y.; Yao, L.; Liu, H.; Zhang, S.; Wang, C.; Shen, F.; Lu, P.; Yang, B.; Ma, Y. A hybridized local and charge-transfer excited state for highly efficient fluorescent oleds: molecular design, spectral character, and full exciton utilization. *Adv. Optical Mater.* **2014**, *2*, 892-901.
- [6] Grabowski, Z. R.; Rotkiewicz, K.; Rettig, W. Structural changes accompanying intramolecular electron transfer: focus on twisted intramolecular charge-transfer states and structures. *Chem. Rev.* **2003**, *103*, 3899-4031.
- [7] Wang, Y.; Xu, D.; Gao, H.; Wang, Y.; Liu, X.; Han, A.; Zhang, C.; Zang, L. Mechanofluorochromic properties of aggregation-induced emission-active tetraphenylethene-containing cruciform luminophores. *Dyes. Pigments.* **2018**, *156*, 291-298.
- [8] Yu, T.; Ou, D.; Wang, L.; Zheng, S.; Yang, Z.; Zhang, Y.; Chi, Z.; Liu, S.; Xua, J.; Aldred, M. P. A new approach to switchable photochromic materials by combining photochromism and piezochromism together in an AIE-active molecule. *Mater. Chem. Front.* **2017**, *1*, 1900-1904.
- [9] Shan, G.; Li, H.; Zhu, D.; Su, Z.; Liao, Y. Intramolecular π -stacking in cationic iridium(III) complexes with a triazole-pyridine type ancillary ligand: synthesis, photophysics, electrochemistry properties and piezochromic behavior. *J. Mater. Chem.* **2012**, *22*, 12736-12744.
- [10] Huang, G.; Jiang, Y.; Yang, S.; Li, B.; Tang, B. Multistimuli response and polymorphism of a novel tetraphenylethylene derivative. *Adv. Funct. Mater.* **2019**, *29*, 1900516-1900524.

- [11] Zhang, Y.; Wang, K.; Zhuang, G.; Xie, Z.; Zhang, C.; Cao, F.; Pan, G.; Chen, H.; Zou, B.; Ma, Y. Multicolored-fluorescence switching of ICT-Type organic solids with clear color difference: mechanically controlled excited state. *Chem. Eur. J.* **2015**, *21*, 2474 -2479.
- [12] Zhang, G.; Yang, G.; Wang, S.; Chen, Q.; Ma, J. S. A highly fluorescent anthracene - containing hybrid material exhibiting tunable blue-green emission based on the formation of an unusual “T - shaped” excimer. *Chem. Eur. J.*, **2007**, *13*, 3630-3635.
- [13] Wang, K.; Zheng, C.; Liu, W.; Liang, K.; Shi, Y.; Tao, S.; Lee, C.; Ou, X.; Zhang, X. Avoiding energy loss on TADF emitters: controlling the dual conformations of D-A structure molecules based on the pseudoplanar segments. *Adv. Mater.* **2017**, *19*, 1701476-1701484.
- [14] Xie, Z.; Yu, T.; Chen, J.; Ubba, E.; Wang, L.; Mao, Z.; Su, T.; Zhang, Y.; Aldred, M. P.; Chi, Z. Weak interactions but potent effect: tunable mechanoluminescence by adjusting intermolecular C-H $\cdots\pi$ interactions. *Chem. Sci.* **2018**, *9*, 5787-5794
- [15] Zhang, Y.; Qile, M.; Sun, J.; Xu, M.; Wang, K.; Cao, F.; Li, W.; Song, Q.; Zou, B.; Zhang, C. Ratiometric pressure sensors based on cyano-substituted oligo(*p*-phenylene vinylene) derivatives in the hybridized local and charge-transfer excited state. *J. Mater. Chem. C*, **2016**, *4*, 9954-9960.
- [16] Li, W.; Wang, S.; Zhang, Y.; Gao, Y.; Dong, Y.; Zhang, X.; Song, Q.; Yang, B.; Ma, Y.; Zhang, C. Highly efficient luminescent *E*- and *Z*-isomers with stable configurations under photoirradiation induced by their charge transfer excited states. *J. Mater. Chem. C* **2017**, *5*, 8097-8104.

- [17] Shen, X.; Wang, Y.; Zhao, E.; Yuan, W.; Liu, Y.; Lu, P.; Qin, A.; Ma, Y.; Sun, J.; Tang, B. Effects of substitution with donor–acceptor groups on the properties of tetraphenylethene trimer: aggregation-induced emission, solvatochromism, and mechanochromism. *J. Phys. Chem. C* **2013**, *117*, 7334–7347.
- [18] Zhang, Y.; Zhang, J.; Shen, J.; Sun, J.; Wang, K.; Xie, Z.; Gao, H.; Zou, B. Solid-state TICT-emissive cruciform: aggregation-enhanced emission, deep-red to near-infrared piezochromism and imaging in vivo. *Adv. Optical Mater.* **2018**, *6*, 180956-1800966.
- [19] Chen, C.; Huang, R.; Batsanov, A. S.; Pande, r P.; Hsu, Y.-T.; Chi, Z.; Dias, F. B.; Bryce, M. R. Intramolecular charge transfer controls switching between room temperature phosphorescence and thermally activated delayed fluorescence. *Angew. Chem.* **2018**, *130*, 16645-16649.
- [20] Yang, J.; Qin, J.; Geng, P.; Wang, J.; Fang, M.; Li, Z. Molecular conformation-dependent mechanoluminescence: same mechanical stimulus but different emissive color over time. *Angew. Chem. Int. Ed.* **2018**, *57*, 14174-14178.
- [21] Yu, Y.; Zhao, R.; Zhou, C.; Sun, X.; Wang, S.; Gao, Y.; Li, W.; Lu, P.; Yang, B.; Zhang, C. Highly efficient luminescent benzoylimino derivative and fluorescent probe from a photochemical reaction of imidazole as an oxygen sensor. *Chem. Commun.* **2019**, *55*, 977-980.
- [22] Zhang, S.; Dai, Y.; Luo, S.; Gao, Y.; Gao, N.; Wang, K.; Zou, B.; Yang, B.; Ma, Y. Rehybridization of nitrogen atom induced photoluminescence enhancement under pressure stimulation. *Adv. Funct. Mater.* **2017**, *27*, 1602276.

- [23] Li, A.; Ma, Z.; Wu, J.; Li, P.; Wang, H.; Geng, Y.; Xu, S.; Yang, B.; Zhang, H.; Cui, H.; Xu, W. Pressure-induced wide-range reversible emission shift of triphenylamine-substituted anthracene via hybridized local and charge transfer (HLCT) excited state. *Adv. Optical Mater.* **2018**, *6*, 1700647-1700655.
- [24] Shillito, G. E.; Hall, T. B. J.; Preston, D.; Traber, P.; Wu, L.; Reynolds, K. E. A.; Horvath, R.; Sun, X. Z.; Lucas, N. T.; Crowley, J. D.; George, M. W.; Kupfer, S.; Gordon, K. C. Dramatic alteration of ³ILCT lifetimes using ancillary ligands in [Re(L)(CO)₃(phen-TPA)]ⁿ⁺ complexes: an integrated spectroscopic and theoretical study. *J. Am. Chem. Soc.* **2018**, *140*, 4534–4542.
- [25] Lv, X.; Yan, S.; Dai, Y.; Ouyang, M.; Yang, Y.; Yu, P.; Zhang, C. Ion diffusion and electrochromic performance of poly(4,4',4''-tris[4-(2-bithienyl)phenyl]amine) based on ionic liquid as electrolyte. *Electrochim. Acta.* **2015**, *186*, 85–94.
- [26] Chen, Z.; Su, C.; Zhu, X.; Xu, R.; Xu, L.; Zhang, C. Micro-/mesoporous conjugated polymer based on star-shaped triazine-functional triphenylamine framework as the performance-improved cathode of Li-organic battery. *J. Polym. Sci. Pol. Chem.* **2018**, *22*, 2574-2583.
- [27] Feng, J. K.; Cao, Y. L.; Ai, X. P.; Yang, H. X. Polytriphenylamine: A high power and high capacity cathode material for rechargeable lithium batteries. *J. Power Sources.* **2008**, *177*, 199–204.
- [28] Dong, Y.; Xu, B.; Zhang, J.; Tan, X.; Wang, L.; Chen, J.; Lv, H.; Wen, S.; Li, B.; Ye, L.; Zou, B.; Tian, W. Piezochromic luminescence based on the molecular aggregation of 9,10-bis((e)-2-(pyrid-2-yl)vinyl) anthracene. *Angew. Chem. Int. Ed.* **2012**, *51*, 10782-10785.

- [29] Qi, Y.; Ding, N.; Wang, Z.; Xu, L.; Fang, Y. Mechanochromic wide-spectrum luminescence based on a monoboron complex. *ACS Appl. Mater. Interfaces*. **2019**, *11*, 8676-8684.
- [30] Xiong, J.; Wang, K.; Yao, Z.; Zou, B.; Xu, J.; Bu, X. Multi-stimuli-responsive fluorescence switching from a pyridine-functionalized tetraphenylethene aiegen. *ACS Appl. Mater. Interfaces*. **2018**, *10*, 5819–5827.
- [31] Chi, Z.; Zhang, X.; Xu, B.; Zhou, X.; Ma, C.; Zhang, Y.; Liu, S.; Xu, J. Recent advances in organic mechanofluorochromic materials. *Chem. Soc. Rev.* **2012**, *41*, 3878–3896.
- [32] Li, H.; Chi, Z.; Xu, B.; Zhang, X.; Li, X.; Liu, S.; Zhang, Y.; Xu, J. Aggregation-induced emission enhancement compounds containing triphenylamine-anthrylenevinylene and tetraphenylethene moieties. *J. Mater. Chem.* **2011**, *21*, 3760–3767.
- [33] Seki, T.; Tokodai, N.; Omagari, S.; Nakanishi, T.; Hasegawa, Y.; Iwasa, T.; Taketsugu, T.; Ito, H. Luminescent mechanochromic 9-anthryl Gold(I) isocyanide complex with an emission maximum at 900 nm after mechanical stimulation. *J. Am. Chem. Soc.*, **2017**, *139*, 6514-6517.

Figure Caption

Figure 1. Molecular structures of DPA-PYZ and TPA-PYZ as well as their optimized molecular configurations in the ground state.

Figure 2. (a) PL spectra of DPA-PYZ and TPA-PYZ films and solutions (THF, 10⁻⁵ M). (b) PL spectra of DPA-PYZ and TPA-PYZ single crystals. Inset photo show the crystals under UV light in dark Figure Caption.

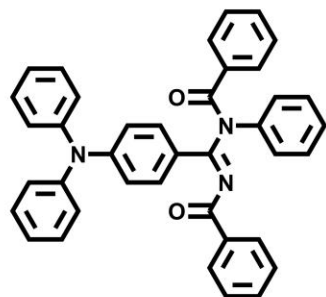
Figure 3. Single crystal structures of DPA-PYZ and TPA-PYZ. (The right is the simplified molecular structure.)

Figure 4. The calculated natural transition orbitals (hole and particle) and the corresponding excitation energy of DPA-PYZ molecule with the different twist angles between DPA donor and PYZ acceptor for the S₀→S₁ excitation at td-m062x/6-31g (d, p) level using the geometry of the S₀ state where td represents time-dependent density functional theory (TDDFT).

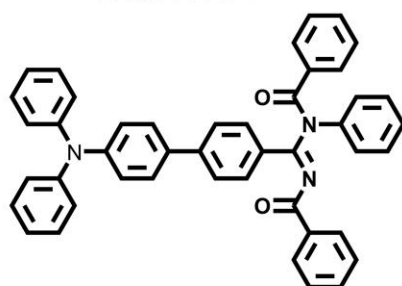
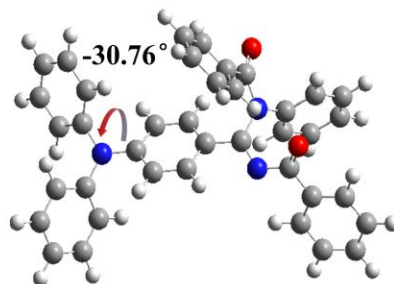
Figure 4. Raman spectra at the selected range for the yellow-emission and blue-emission DPA-PYZ powders. (The excitation wavelength of the Raman spectra is 632 nm).

Figure 5. (a) The diagram of DPA-PYZ with different D-A structure distortions and illuminations in the solid state; (b) Photos of DPA-PYZ under UV irradiation in powder states (I, grinding; II, fuming with DCM vapor or annealing under 60 °C). (c) Normalized PL spectra of blue-emissive crystalline DPA-PYZ powder under mechanical grinding: crystalline powder, slightly grinded, deficiently grinded, and fully grinded. (d) Normalized PL spectra of yellow-emissive amorphous DPA-PYZ powder under annealing under 60 °C by rapid evaporation of the DPA-PYZ dichloromethane solution.

Figure1 (1/6)



DPA-PYZ



TPA-PYZ

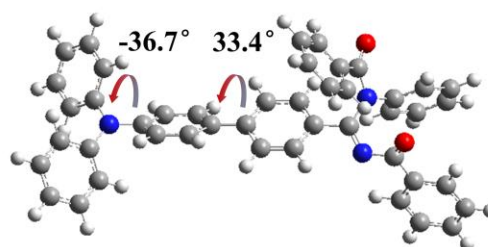


Figure2 (2/6)

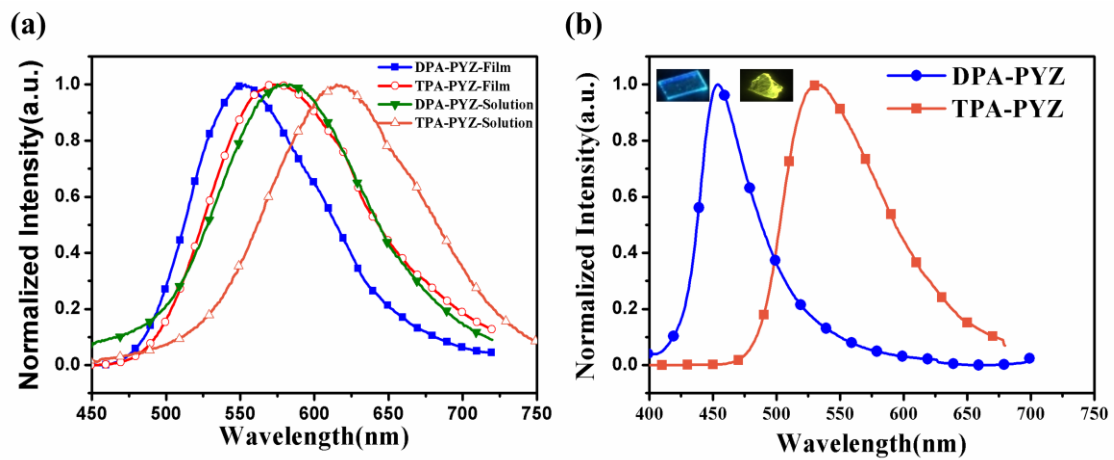


Figure3 (3/6)

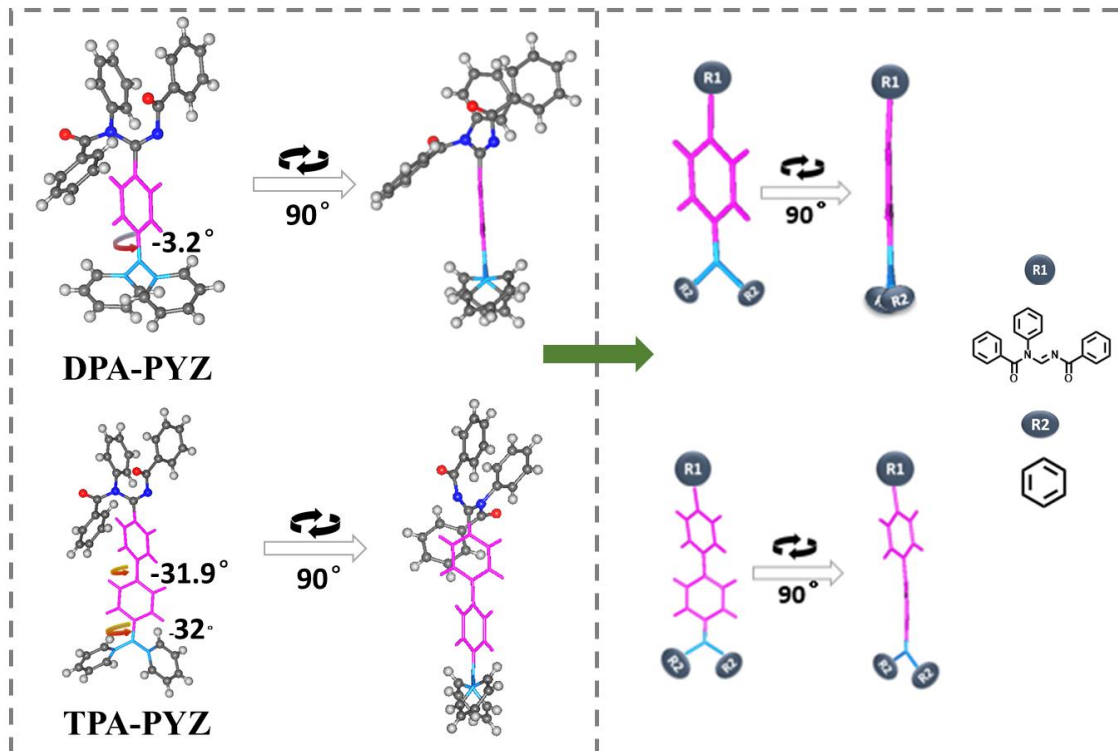


Figure4 (4/6)

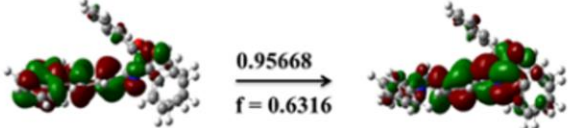
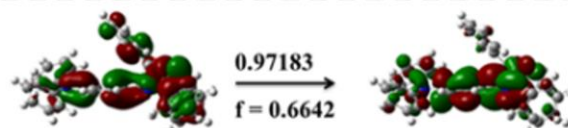
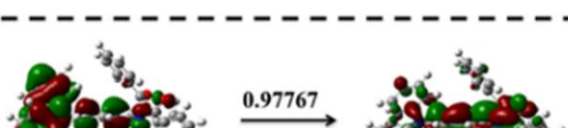
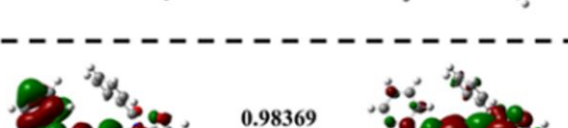
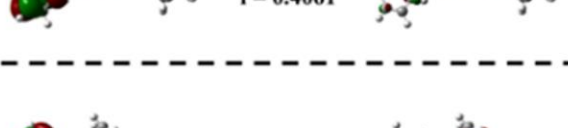
Twist angle	“Hole” \longrightarrow “Particle”	Excitation energy (eV)
1°	 $\xrightarrow[0.95668]{f = 0.6316}$	3.22
19°	 $\xrightarrow[0.97183]{f = 0.6642}$	3.05
39°	 $\xrightarrow[0.97767]{f = 0.5785}$	2.95
59°	 $\xrightarrow[0.98369]{f = 0.4061}$	2.91
81°	 $\xrightarrow[0.99752]{f = 0.0019}$	2.84

Figure5 (5/6)

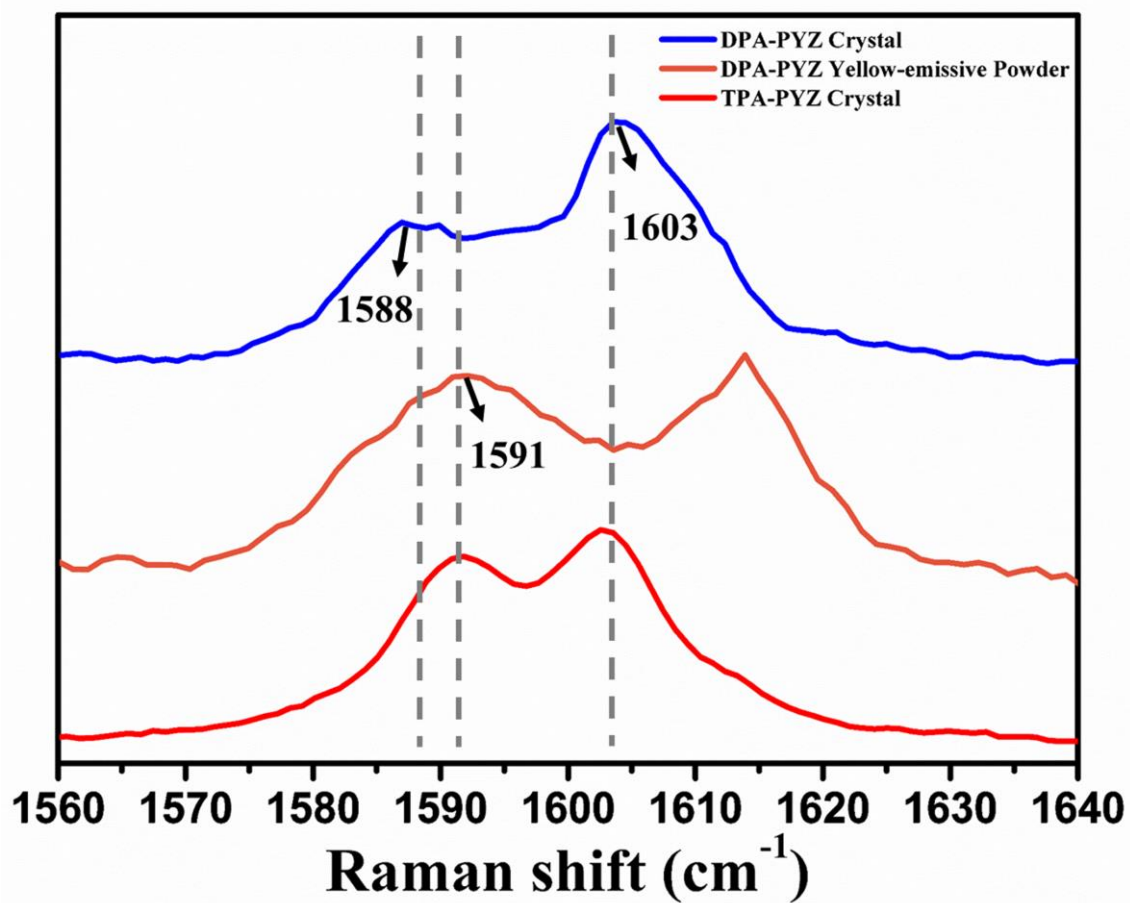
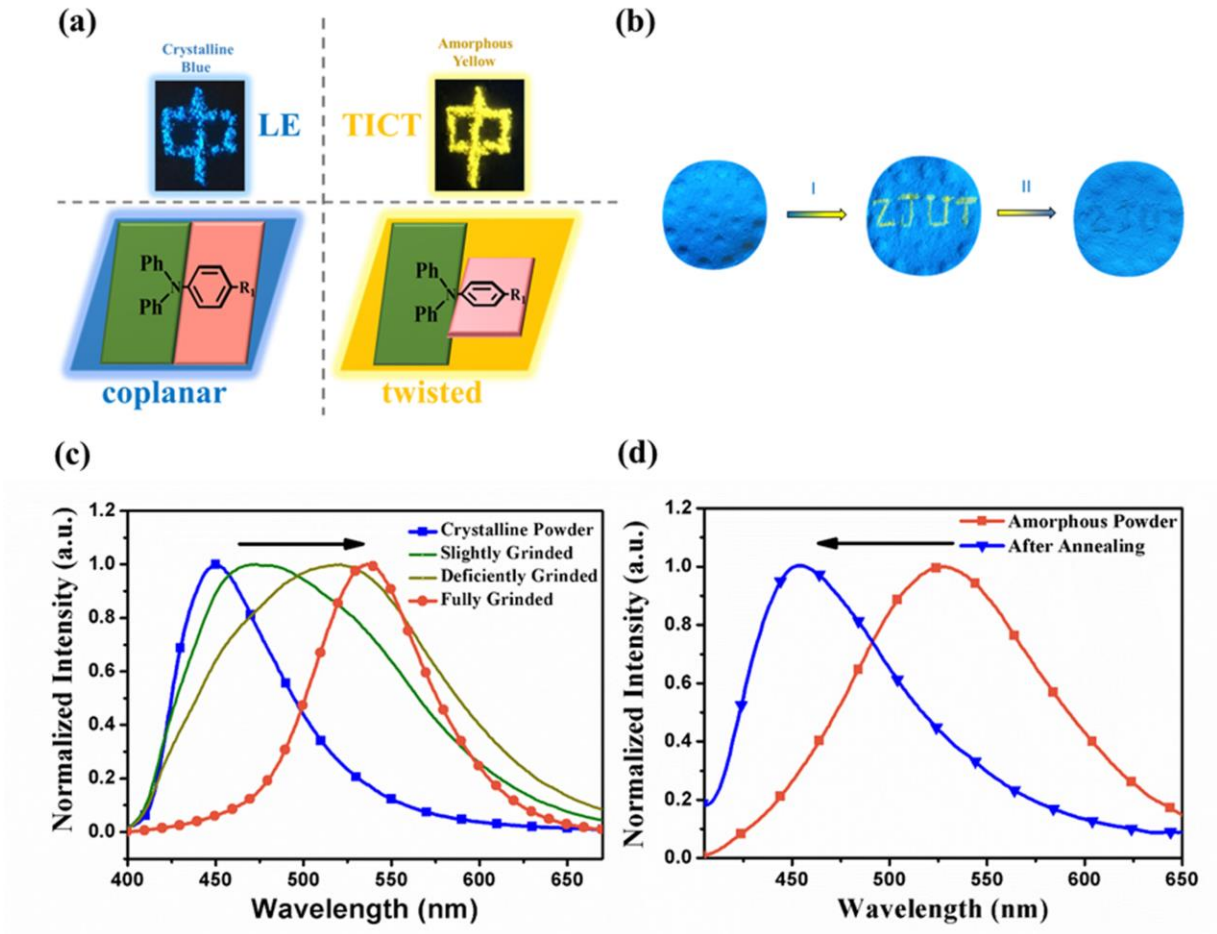


Figure6 (6/6)



Supporting Information

Direct Observation of Excited State Conversion in Solid State from a TICT-Type Mechanochromic Luminogen

Jianai Chen¹, Sijie Tan¹, Yue Yu¹, Shitong Zhang², Weijun Li¹, Qingbao Song¹, Yujie Dong^{1*},
Cheng Zhang^{1*}, and Wai-Yeung Wong^{3*}

¹State Key Laboratory Breeding Base of Green Chemistry Synthesis Technology, College of Chemical Engineering, Zhejiang University of Technology, Hangzhou 310014, P. R. China.

²State Key Lab of Supramolecular Structure and Materials, Jilin University, 2699 Qianjin Avenue, Changchun 130012, P. R. China.

³Department of Applied Biology & Chemical Technology, The Hong Kong Polytechnic University, Hung Hom, Hong Kong, P. R. China; Hong Kong Polytechnic University Shenzhen Research Institute, Shenzhen 518057, P.R. China.

Corresponding authors: dongyujie@zjut.edu.cn, czhang@zjut.edu.cn and wai-yeung.wong@polyu.edu.hk

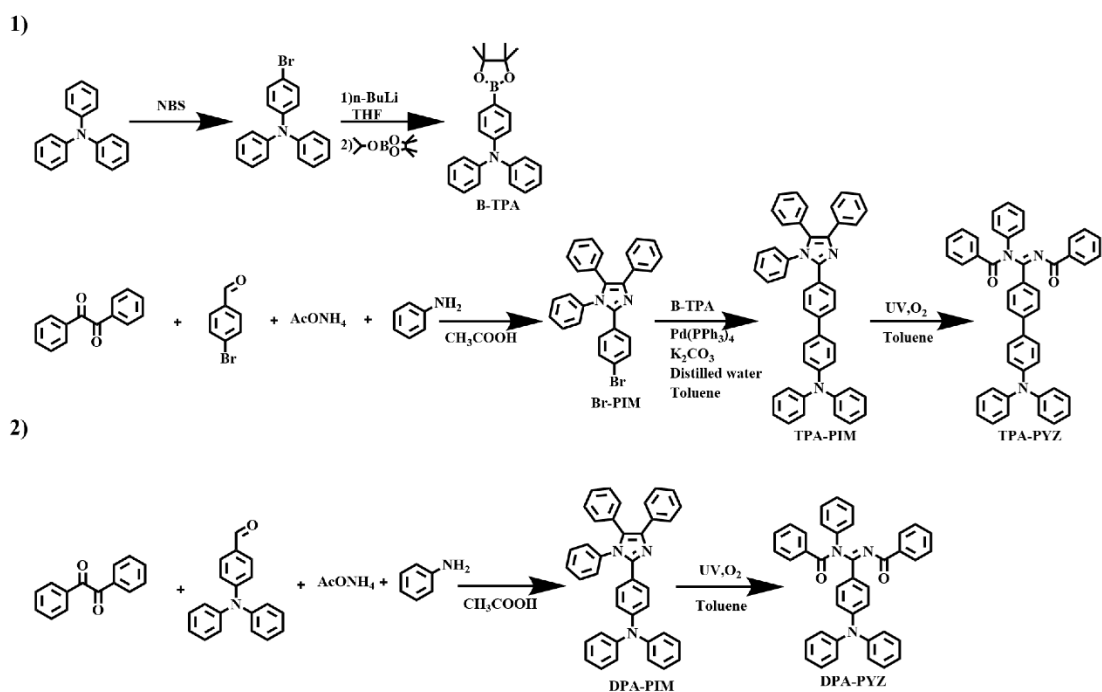
Supporting Information

Contents

- 1. Synthesis**
- 2. DFT, PL and UV spectra of DPA-PYZ and TPA-PYZ**
- 3. Molecular packing of DPA-PYZ and TPA-PYZ**
- 4. Lifetime measurement of DPA-PYZ**
- 5. Mechanochromism Experiments**
- 6. References**

1. Synthesis

All the reagents or chemicals were commercial products without further purification. The preparation procedure of DPA-PIM and TPA-PIM could be found in reference. [1, 2]



Scheme S1. The synthesis of 1) DPA-PYZ and 2) TPA-PYZ

2. DFT, PL and UV spectra of DPA-PYZ and TPA-PYZ

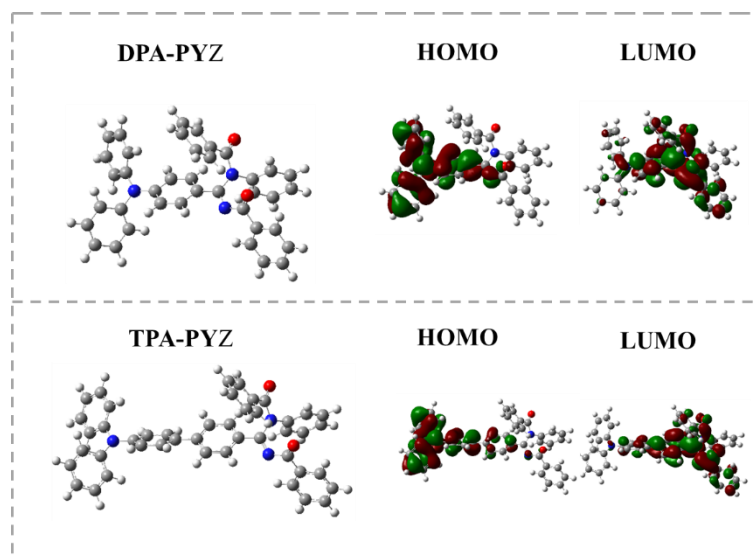


Figure S1. The optimized molecular configurations of DPA-PYZ and TPA-PYZ as well as calculated electronic cloud distributions of frontier orbitals in ground state.

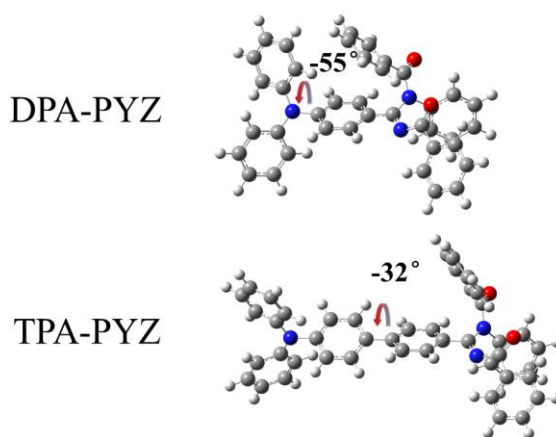


Figure S2. The optimized molecular configurations of DPA-PYZ and TPA-PYZ in the excited state.

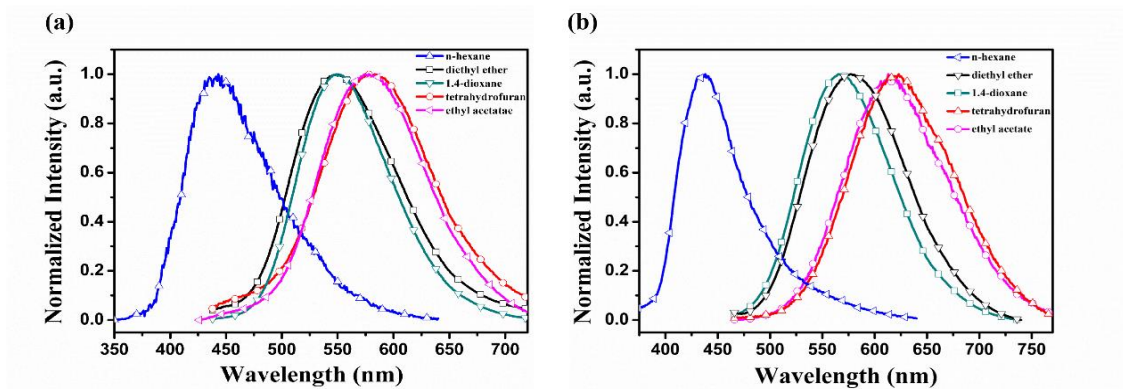


Figure S3. PL spectra of (a) DPA-PYZ and (b) TPA-PYZ measured in different solvents with increasing polarity (n-hexane, diethyl ether, 1, 4-dioxane, tetrahydrofuran and ethyl acetate).

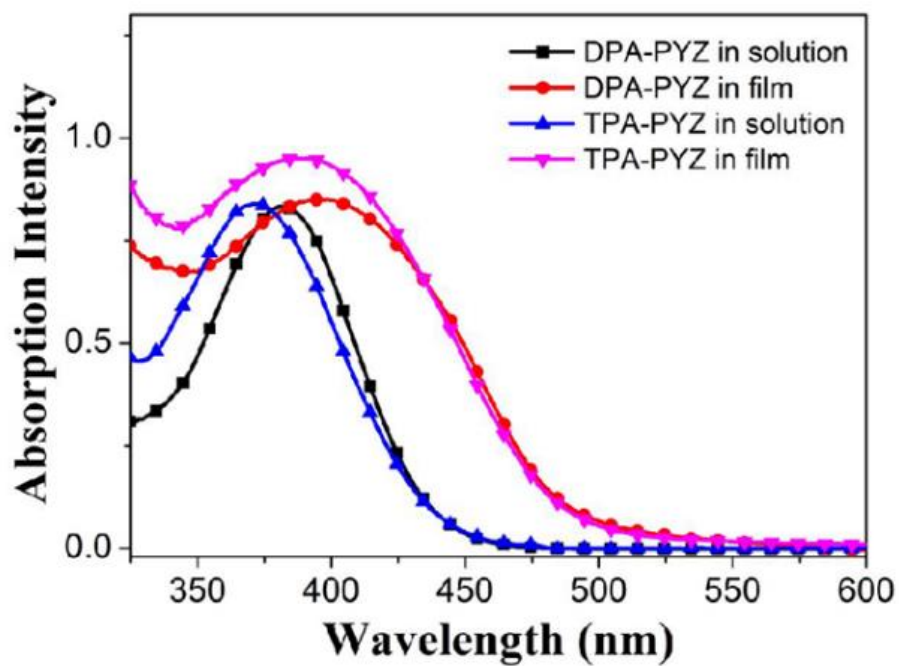
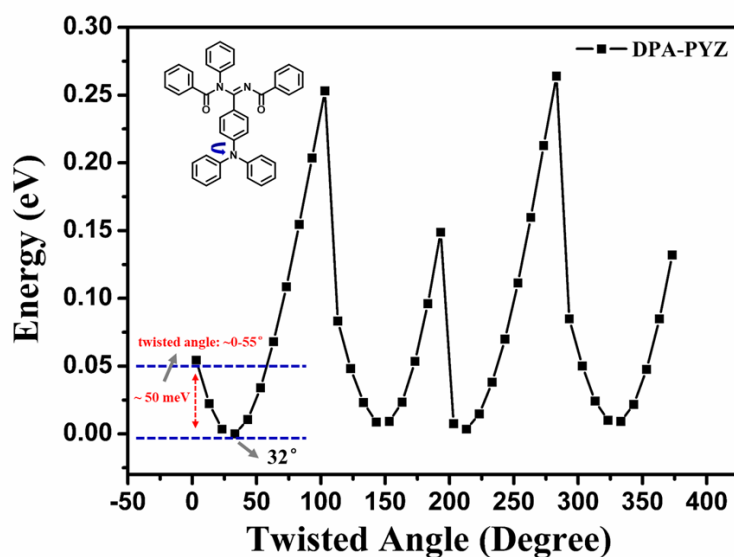


Figure S4. UV spectra of DPA-PYZ and TPA-PYZ measured in solution and film



state.

Fig

re S5. The ground state energy of DPA-PYZ at different twist angles between DPA donor and PYZ acceptor using the b3lyp method.

Twist angle	“Hole” → “Particle”	Excitation energy (eV)
1°	93% f=0.3869	3.0600
19°	91% f=0.3110	3.0948
39°	85% f=0.0198	3.1277
59°	84% f=0.0065	3.1316
81°	84% f=0.0056	3.1323

Figure S6. The calculated natural transition orbitals (hole and particle) and the corresponding excitation energy of TPA-PYZ molecule with the different twist angles between TPA donor and

PYZ acceptor for the $S_0 \rightarrow S_1$ excitation at td-m062x/6-31g (d, p) level using the geometry of the S_0 state where td represents time-dependent density functional theory (TDDFT)

3. Molecular packing of DPA-PYZ and TPA-PYZ

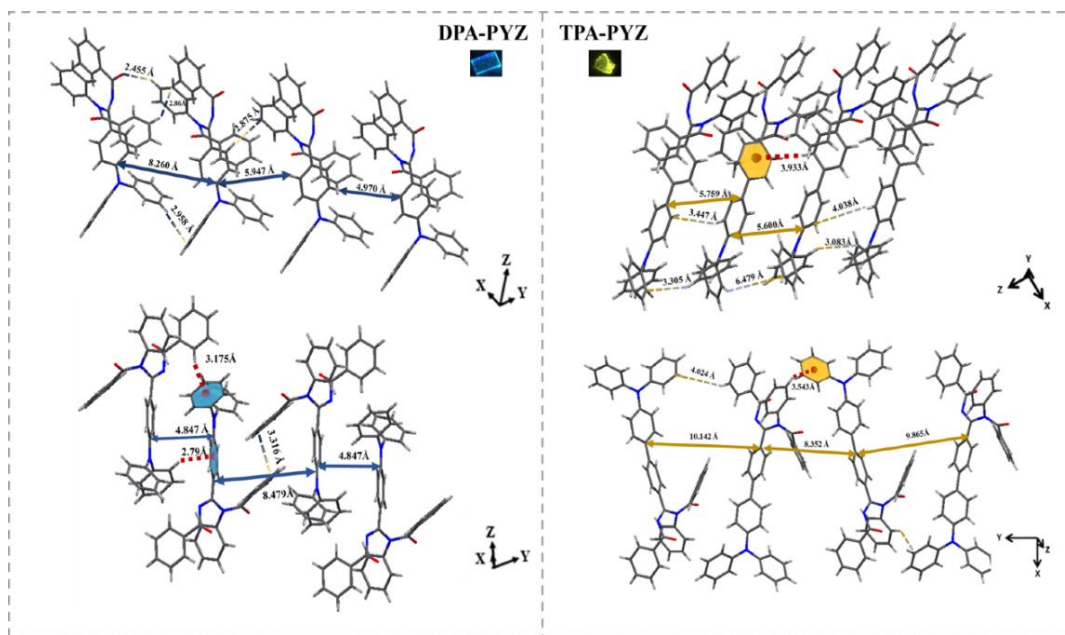


Figure S7. Molecular packing of (a) DPA-PYZ and (b) TPA-PYZ.

4. Lifetime measurement of DPA-PYZ

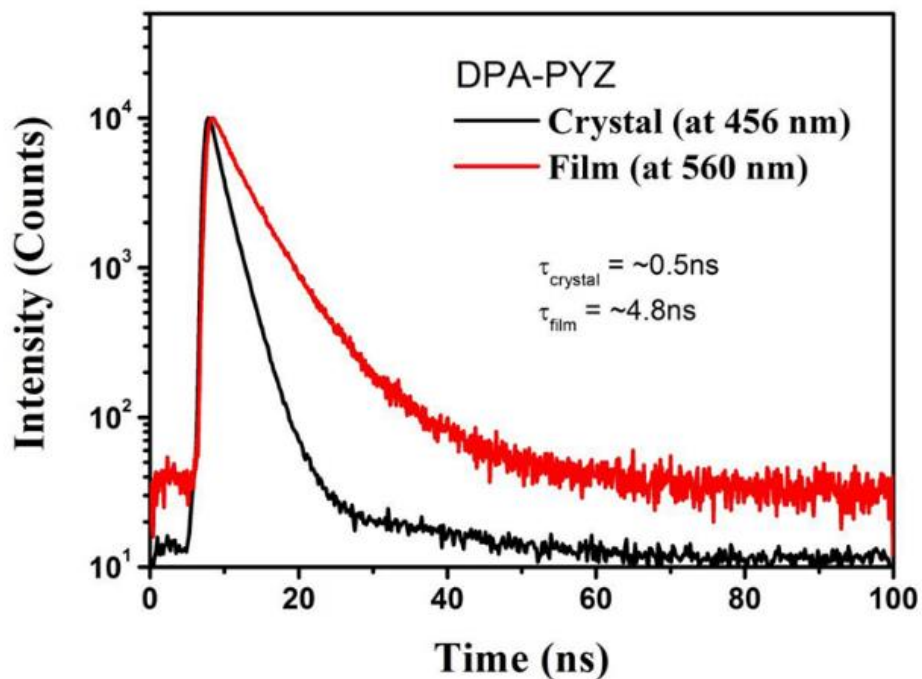


Figure S8. Lifetime measurement of the fluorescence of crystal and film of DPA-PYZ measured at 456 and 560 nm, respectively.

5. Mechanochromism properties.

Table S1. The assignments and frequencies (cm^{-1}) of observed Raman internal modes of DPA-PYZ and TPA-PYZ in comparison with DFT simulation results.

	Experimental value [cm^{-1}]	Theoretical value [cm^{-1}]	Vibrational mode
DPA-PYZ	1588	1640	Breathing vibration of benzene form triphenylamine
	1603	1669	
TPA-PYZ	1591	1660	Breathing vibration of benzene form triphenylamine
	1603	1680	

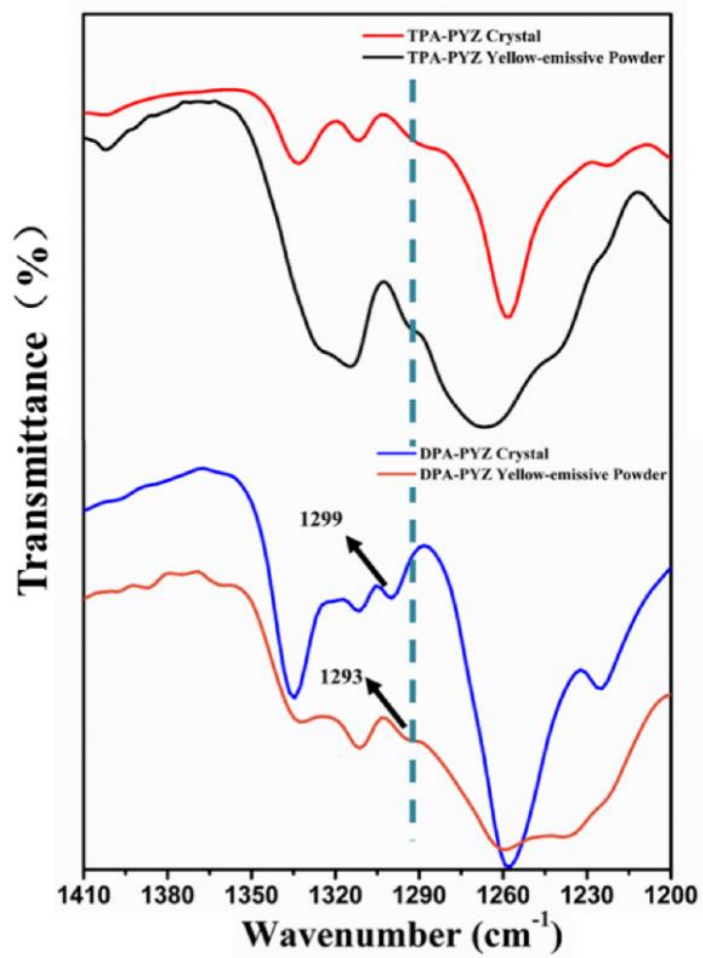


Figure S9. FT-IR spectra of DPA-PYZ and TPA-PYZ in the different solid states.

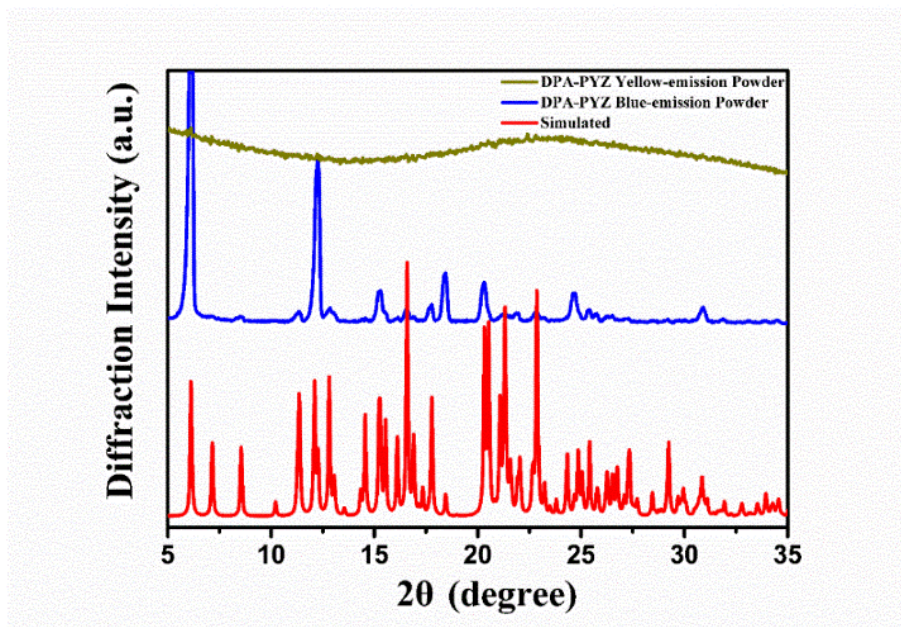
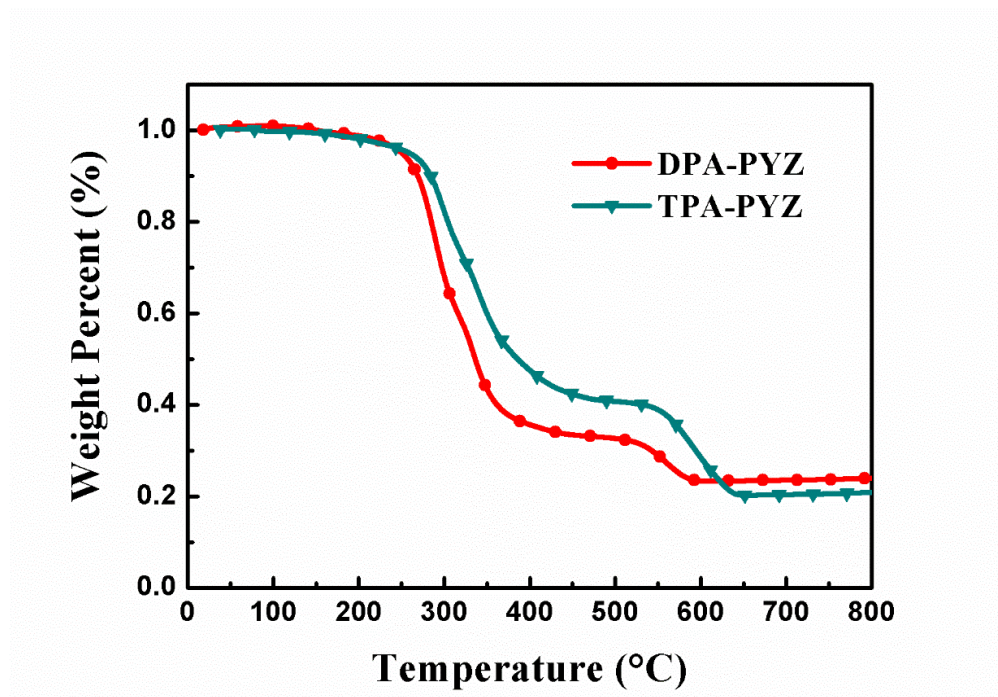


Figure S10. Powder X-ray diffraction (PXRD) data of DPA-PYZ powders with different emission (with that simulated from DPA-PYZ single crystal structure as reference).



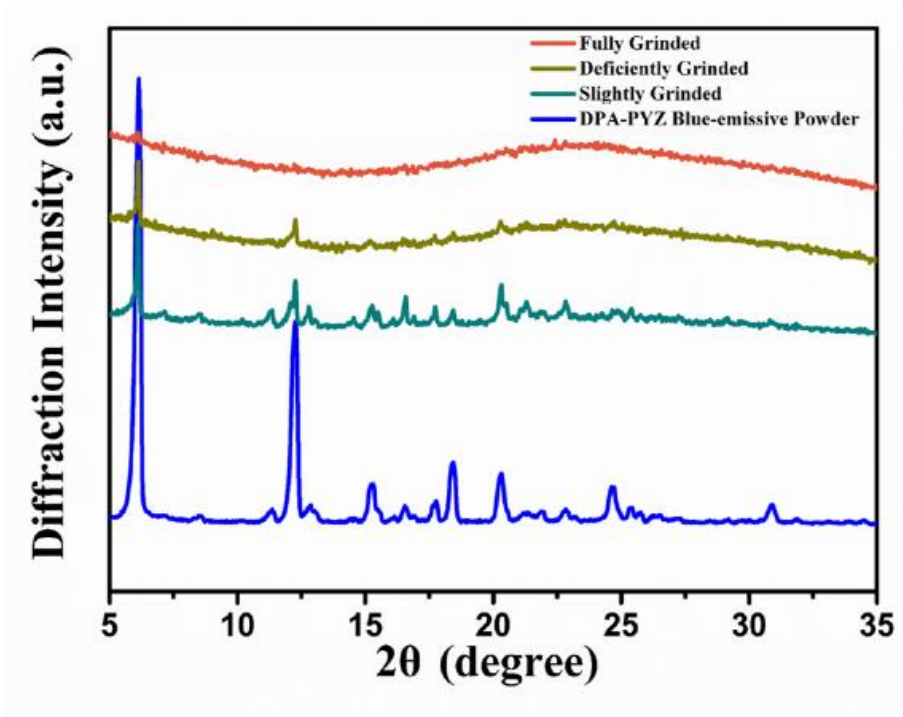


Figure S11. The TG graphs of DPA-PYZ and TPA-PYZ.

Figure S12. Powder X-ray diffraction (PXRD) data of DPA-PYZ in the different solid states.

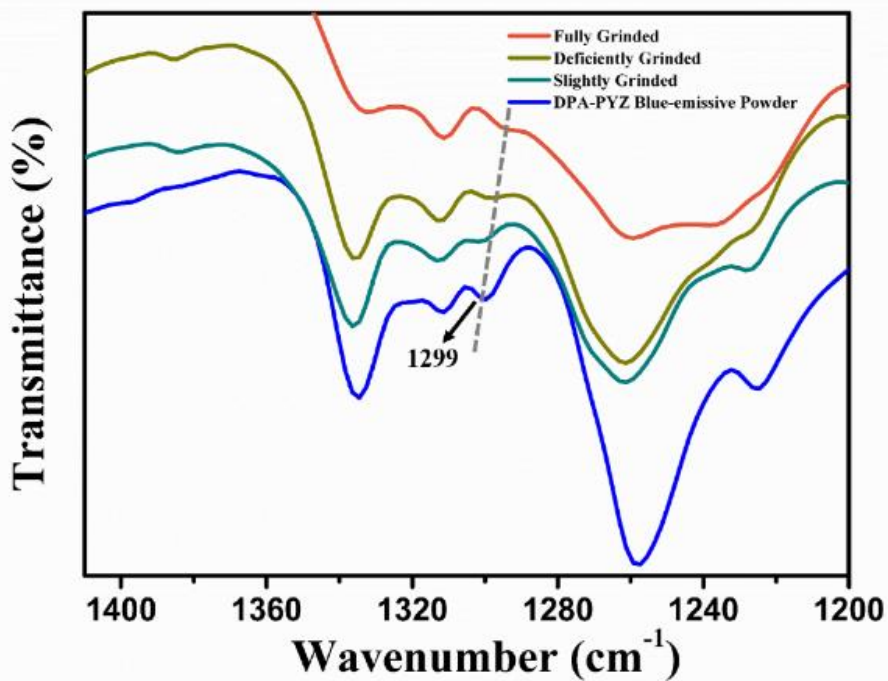


Figure S13. FT-IR spectra of DPA-PYZ in the different solid states.

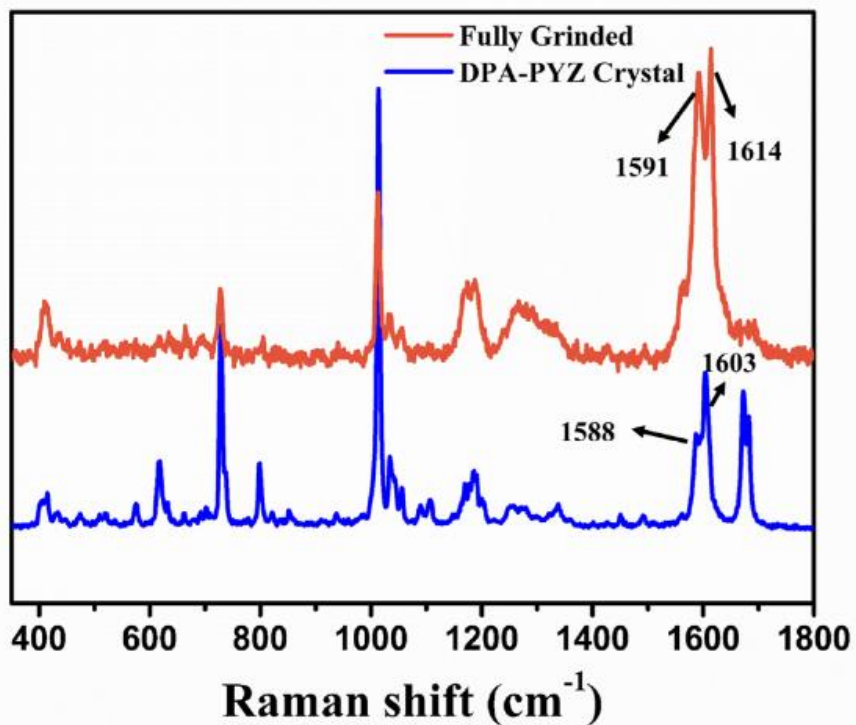


Figure S14. The Raman spectra of DPA-PYZ in the different solid states. (The excitation wavelength of the Raman spectra is 632.81 nm).

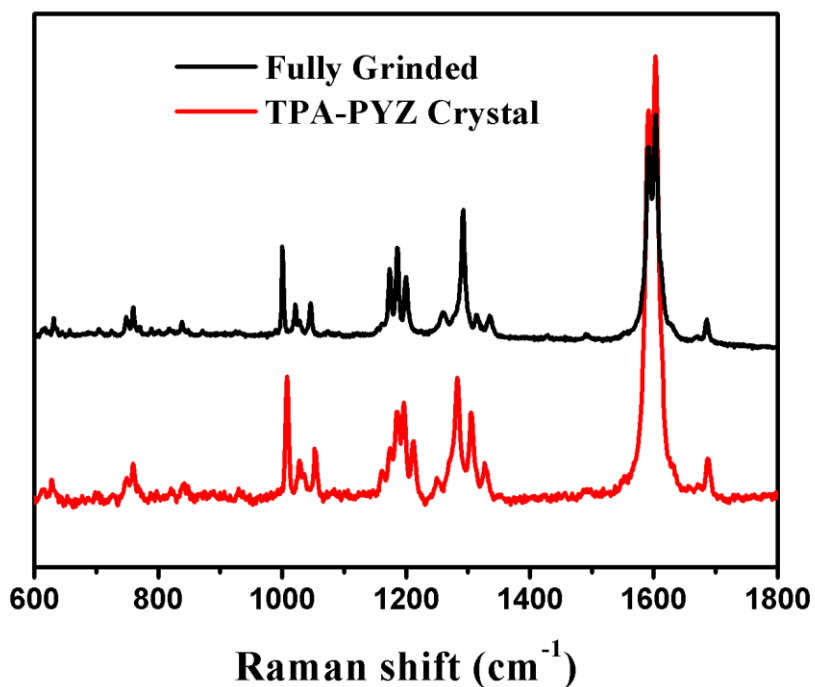


Figure S15. The Raman spectra of TPA-PYZ under mechanical grinding. (The excitation wavelength of the Raman spectra is 632 nm for crystal and 671 nm for grinded sample).

6. References

- (1) Yu, Y.; Zhao, R.; Zhou, C.; Sun, X.; Wang, S.; Gao, Y.; Li, W.; Lu, P.; Yang, B.; Zhang, C. Highly efficient luminescent benzoylimino derivative and fluorescent probe from a photochemical reaction of imidazole as an oxygen sensor. *Chem. Commun.* **2019**, 55, 977-980.

(2) Li, W.; Yao, L.; Liu, H.; Wang, Z.; Zhang, S.; Xiao, R.; Zhang, H.; Lu, P.; Yang, B.; Ma, Y. Highly efficient deep-blue OLED with an extraordinarily narrow FWHM of 35 nm and a y coordinate <0.05 based on a fully twisting donor-acceptor molecule. *J Mater. Chem. C* **2014**, 2, 4733-4736.